Journal of Materials Chemistry C



PAPER

View Article Online



Cite this: DOI: 10.1039/d4tc01281j

Photo-responsive Diels—Alder based azobenzene-functionalized main-chain liquid crystal networks†

Minwook Park, Jesus Guillen Campos, Friedrich Stricker and Javier Read de Alaniz **D**

Light-responsive liquid crystal elastomer networks (LCNs) have received significant interest due to their potential application in soft robotics and shape-morphing devices. Here, we present a systematic examination of light-responsive LCNs prepared using a catalyst-free Diels-Alder cycloaddition and a new azobenzene functionalized monomer for main-chain incorporation. The networks have robust mechanical stiffness that can be reversibly modulated by 1 GPa by turning the UV light on and off. This study highlights the contribution of photothermal softening to reversibly control rheological properties of the newly developed LCNs and demonstrates the ability to tune the modulus on demand. We believe this work will guide future developments of light-responsive LCNs based on the newly developed Diels-Alder cycloaddition.

Received 29th March 2024, Accepted 28th June 2024

DOI: 10.1039/d4tc01281j

rsc.li/materials-c

Introduction, results and discussion, experimental

Liquid crystal networks (LCNs) represent a class of stimuliresponsive materials, offering a unique synergy between molecular order inherent in crystalline materials and elasticity of rubber.^{1,2} LCNs typically consist of two fundamental elements: a crosslinked matrix material that forms the primary elastomer network and responsive molecules that induce beneficial properties in polymers in response to heat,³ pH change,⁴ electrical,⁵ or optical stimuli.⁶ The interplay between the inherent anisotropy of liquid crystals, the network architecture, and the stimuli-responsive motifs introduces a remarkable level of tunability to obtain the desired thermomechanical and dynamic properties of the polymer.⁷

Incorporating photo-responsive molecules into LCNs enables spatial and temporal material responses, as well as modulation in the material's structure and behaviour corresponding to changes in light intensity, wavelength, or polarization. This adaptability can be controlled by a range of photo-responsive chromophores, including azobenzene, diarylethene, DASA, hydrazone, as well as a number of organic dyes and photothermal agents. Among these, azobenzene (Azo)-derived photoswitches have emerged as particularly versatile and the most widely used molecular motif. This is primarily due to their convenient chemical incorporation into LCNs, chemical tunability, large configurational change and reversible

photoisomerization.¹³ Upon absorbing light of a specific wavelength (typically in the UV region), azobenzene transitions from the thermodynamically stable *trans*-state to the higher energy *cis*-state. This photoinduced isomerization is reversible, and the *cis*-isomer can convert back to the *trans*-isomer through thermal relaxation (T-type) or exposure to a different wavelength of light (P-Type). These properties have contributed to the widespread use of azobenzene-derived photochromes in LCN-based actuators and responsive soft materials.

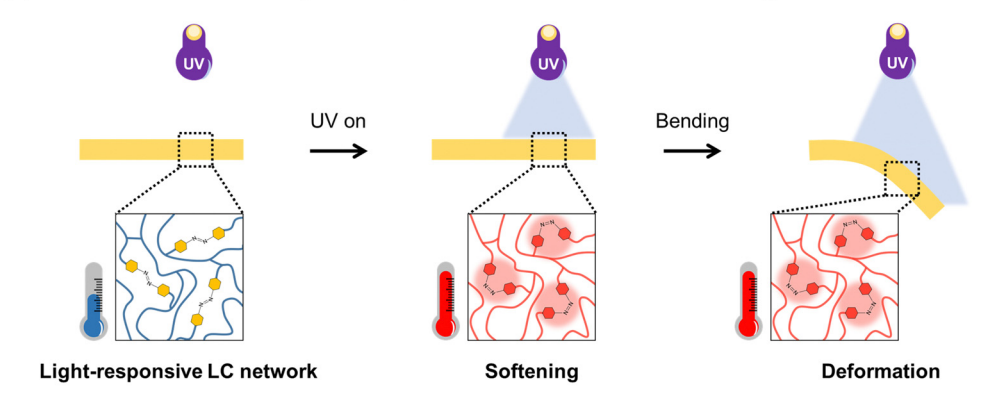
Results

To incorporate azobenzene (Azo) core into the DA-based LCN system, furan-functional groups with a six-methylene chain

Department of Chemistry and Biochemistry, University of California Santa Barbara, Santa Barbara, California 93106, USA. E-mail: javier@chem.ucsb.edu

† Electronic supplementary information (ESI) available. See DOI: https://doi.org/10.1039/d4tc01281j

(a) Schematic illustration of photo-responsive behavior in azo-containing LC network film



(b) Synthesis of Furan-functionalized Azo LC and two types of LC network film

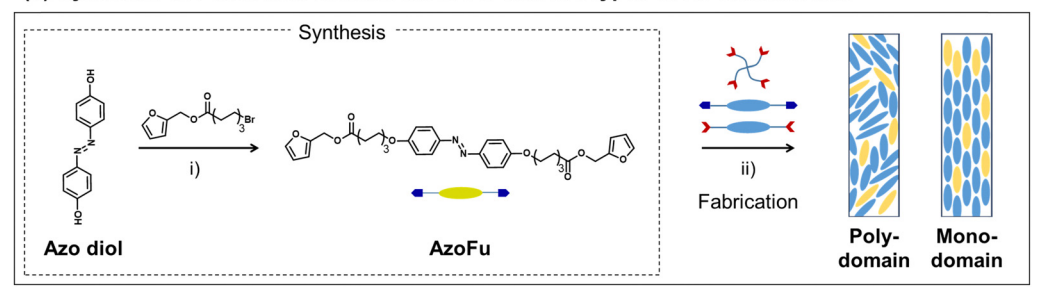


Fig. 1 (a) Photo-responsive behaviour in azo-containing liquid crystal network film (b) synthetic route of furan-functionalized azobenzene liquid crystal (AzoFu) and film fabrication of two types of liquid crystal (LC) network (polydomain and monodomain): (i) K2CO3, KI, DMF, 90 °C, 12 h; (ii) annealed for 7 days at 50 °C, 78 °C, 95 °C respectively in the case of 78 °C, planar surface alignment is used for fabricating monodomain LCN.

spacer were prepared via carbodiimide EDC coupling with the terminal ends of azobenzene-diol (Azo diol) (Fig. 1b). 14 The synthetic procedure and characterization are described in ESI† (Fig. S1 and S2). To evaluate the properties of AzoFu building block, we first examined the thermodynamic behaviour and molecular packing structure using DSC and powder X-ray diffraction (Fig. S3, ESI†). In these experiments, we observed slightly different results in powder samples prepared by solvent-evaporation under vacuum and annealing at 80 $^{\circ}\mathrm{C}$ (Fig. S3a and b, ESI†). 19 In the thermodynamically stable state (annealed), the retention of a broad endothermic peak (84 °C) during repeated heating processes indicates a crystal melting point (T_m) and decent thermal stability. The nematic to isotropic point (T_{ni}) was not observed under these conditions. Given the length of single AzoFu molecule (4.00 nm) and distinct higher order diffraction ((003), (004), (005)), the molecular packing structure of the liquid crystal is expected to possess a smectic A structure with the layer d-spacing of 3.87 nm.²⁰ These results suggest that the AzoFu molecules are uniformly dispersed within the LCN platform and wellaligned along the ordering direction of the matrix LC molecules. In contrast, the powder derived from the solventevaporated state formed a less stable state with closer packed π - π interaction with two distinct d-spacing values (0.31 and 0.30 nm), however no clear higher-order packing structure.

To prepare photo-responsive AzoLCN, we blended monomers in the optimized molar ratios (MFu: 47%, MMal: 43.7%, AzoFu: 5.1%, TMal: 4.2%). The resulting mixture was then used

to fabricate the AzoLCN based on our previous work (Fig. 1(ii)).14 Here, we considered two factors: surface enforced molecular orientation and processing temperature, which can influence the final physical properties and actuation behaviour of the AzoLCN. 21,22 Motivated by these considerations, polydomain films (pAzoLCNs) were prepared at 50 °C, 78 °C, and 95 °C, respectively, while a monodomain film (mAzoLCN) was prepared with a planar surface alignment at 78 °C (nematic phase). The LC properties of these films were characterized by polarized optical microscopy (POM). As expected, there was no optical difference observed by POM for the polydomain AzoLCNs in any direction (Fig. 2a and Fig. S4, ESI†). For the aligned mAzoLCN, we observed a nearly uniform bright texture in the film set at 45° to the polarized optical filters, while no transmitted light was observed at 90°, indicating uniaxially wellaligned molecular orientation.

To investigate the ability to induce photo-responsive deformation in AzoLCN, free-standing cantilevers (13 mm \times 1.3 mm \times 10 μ m) were prepared and monitored under UV and visible light irradiation (Fig. 2b and Fig. S5, ESI†). It is well known that the azobenzene's isomerization (trans-cis) can enhance nanoscale voids in the glassy LCN, thereby inducing volume distribution that leads to macroscopic deformation (expansion/contraction).23 Upon UV light irradiation (20 mW cm⁻²) for 3 minutes, the glassy pAzoLCN quickly bent away from the UV light; however, it did not return to its original shape after UV light irradiation was stopped. Additionally, the pAzoLCN remained unchanged after subsequent visible light irradiation (3 minutes). During 5 cycles alternating between UV and visible light irradiation, the pAzoLCN continued to bend down,

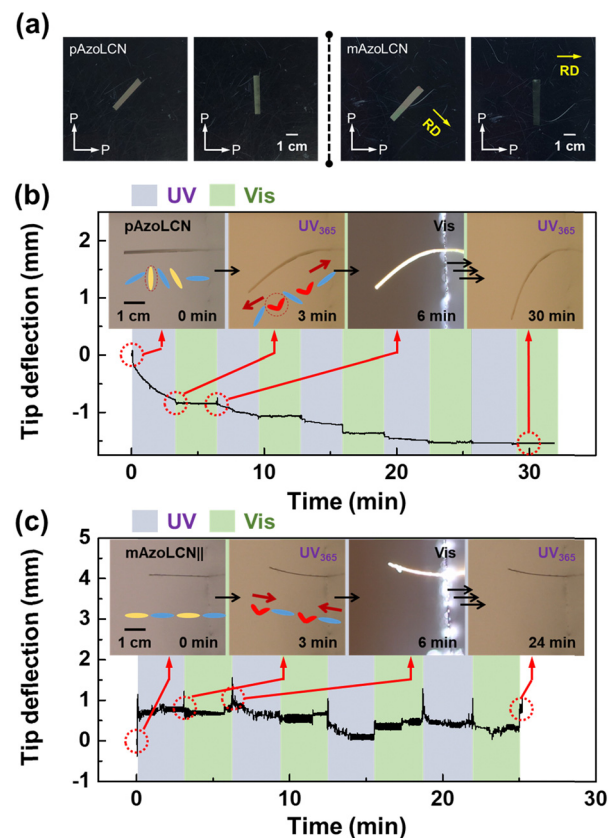


Fig. 2 (a) POM images of polydomain AzoLCN (pAzoLCN) and monodomain AzoLCN (mAzoLCN) under the crossed-polarizers (*P*: polarizer direction). Tip deflection tracking for photo-responsive actuating behaviour of (b) pAzoLCN and (c) mAzoLCN|| under alternative UV or visible light irradiation each for 3 minutes. Inset are the images of the photo-responsive actuating behaviour at each point.

resulting in a -4.5 mm end tip deflection (inset of Fig. 2b). The other pAzoLCN cantilevers prepared at different temperatures (at 50 °C for pAzoLCN50 and at 95 °C for pAzoLCN95) showed similar deformation behaviour with the same bending direction (Fig. S5, ESI†).

In the case of aligned mAzoLCNs (perpendicular alignment = mAzoLCN \(\preceq \) and parallel alignment = mAzoLCN \(|| \), bending behaviour was influenced by the molecular alignment direction (= molecular long axis) (Fig. S5, ESI†).²¹ For example, the upper surface of mAzoLCN \(\preceq \) contracted parallel to molecular long axis and curled slightly upwards. However, the whole cantilever still bent away from the UV source, similar to the behaviour observed in pAzoLCN. In contrast, the mAzoLCN|| cantilever bent toward the UV source, consistent with a buildup of the cis isomer at the surface nearest the light, disrupting the order of the LCN (Fig. 2c). This leads to macroscopic deformation, observed as bending toward the light. There was no additional change beyond 3 minutes, presumably due to gravity. To test this hypothesis, the pAzoLCN cantilever was hung parallel to the direction of gravity. In this configuration, exposure to UV light from the right side of the cantilever caused bending away from the source (Fig. S6, ESI†). Overall, the observed bending angles for the pAzoLCN and mAzoLCN are consistent with

a free-volume change and anisotropy-change, respectively (Fig. S7, ESI†).

To gain a better understanding of the photo-responsive behaviour of both the poly- and mono-domain cantilevers, we examined the kinetics of trans-cis-trans isomerization through time-resolved UV-vis spectra using LCN films (Fig. 3a). Under constant UV light irradiation, the π - π * absorption peak at 360 nm decreased by approximately 45%, reaching steady state after 15 minutes. The metastable cis-isomer can be converted back to the trans-isomer within 4 seconds upon exposure to visible light. In the absence of light, the metastable cis-isomer gradually returns to the trans-form in the dark, reaching 66% recovery after 10 minutes (Fig. 3b). Based on these results, we believe that the main-chain azobenzene photoswitch undergoes efficient switching between trans- and cis-isomers upon UV and Vis light irradiation. However, when investigating the mechanical properties (vide infra), we find that recovery of the modulus in the dark is on the order of seconds. The large mismatch between the relatively slow cis-to-trans-reversed isomerization of azobenzene molecules in the dark and the fast modulus change of the polymer when the light is turned off suggest the dynamics of the trans-to-cis and cis-to-trans isomerization process is decoupled from the driving forces contributing to the macroscopic change in the material properties.

Given these observations, we next investigated the photothermal effect using an IR camera (Fig. 3b). The temperature of AzoLCN immediately increased from 20 °C to 35 °C (ΔT = 15 °C) within 1 second and this temperature is maintained (± 2 °C) during the entire UV light irradiation (17 minutes). For comparison, the temperature change (ΔT) of an LCN sample with no azobenzene was only 5 °C (Fig. S8, ESI†). Prior reports have suggested that azobenzene can generate remarkable local

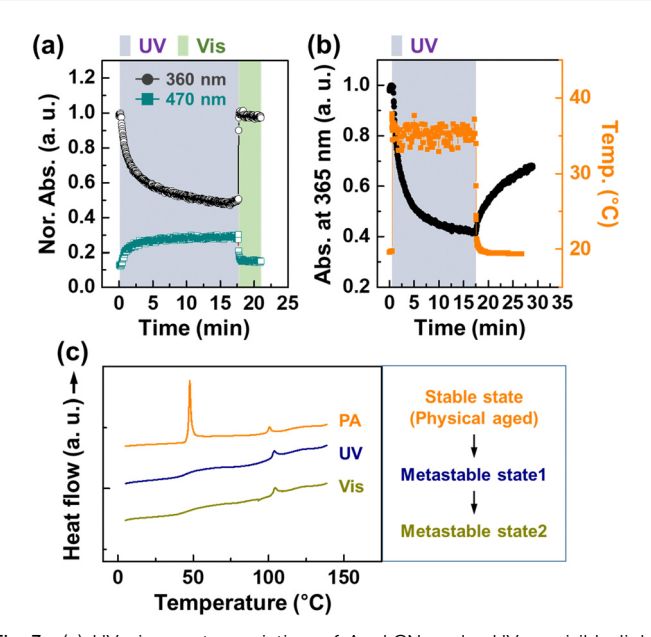


Fig. 3 (a) UV-vis spectra variation of AzoLCN under UV or visible light irradiation. (b) Temperature and absorption (365 nm) variation of AzoLCN before and after UV light irradiation. (c) A set of DSC heating data of AzoLCN at 5 $^{\circ}$ C min $^{-1}$.

effective temperature heating (up to nearly 200 °C).²⁴ We speculate that the local temperature near to azobenzene molecules is also much higher than the recorded bulk surface temperature of 35 °C, which might explain this photothermal softening.

Based on these findings, we further investigated the photothermal effect using differential scanning calorimetry (DSC) in pAzoLCN films (Fig. 3c). A sharp endothermic peak at 48 °C was observed during the first heating process, suggesting the existence of crystallization peak and a physically aged state.²⁵ This physically aged (PA) state is not observed during the second heating process, but is restored if the sample is held below glass transition temperature (T_g) for approximately 2 days (Fig. S9, ESI†). We postulate that the PA state is thermodynamically stable state, which might arise from the differences in the glassy molecular packing between the mesogens, alkyl chains and the Diels-Alder functionalized backbone. Overall, the T_g was observed around 48 °C and nematic-isotropic transition (T_{ni}) of AzoLCN was observed around 100 °C. It is noteworthy that this overlaps with retro-Diels-Alder reaction temperature (100-130 °C), which might decrease cross-linking density if temperatures are held above this temperature.²⁶ Indeed, when the sample is heated above T_{ni} , we observe a lower $T_{\rm g}$ (= 40 °C) peak, which is attributed to the gradual reorganization of molecular packing and a small population of the DA adducts undergoing bond breaking through the retro-DA cycloaddition. This would lower the cross-linking density and decrease T_g . Consistent with the photothermal effects observe upon UV irradiation, the PA state was not observed upon exposure to UV light for 10 minutes (Fig. 3c; blue graph). When AzoLCN was exposed to UV light for 10 minutes and subsequently visible light for 1 minute, it exhibited the same thermogram as the AzoLCN solely exposed to UV light. Additionally, the global molecular packing structure in the Azo-LCN remained unchanged before and after UV light irradiation (Fig. S10, ESI†).

To investigate the impact of photothermal and photochemical effects on the mechanical properties of the LCN, we monitored the storage (G') and loss (G'') moduli using DMA under UV and visible light irradiation (Fig. 4a and c). Upon UV light irradiation, the storage modules decreased almost immediately from \sim 2 GPa to \sim 1 GPa. Likewise, the loss modulus increased from 60 to 300 MPa (Fig. 4a). The G' and G'' were maintained with similar values under irradiation (2 minutes). When the UV light was turned off, these values quickly returned to the initial value in approximately 6 seconds. Given the slow *cis-trans* back isomerization in the dark (Fig. 2b), we attribute this change to photothermal softening. Similar results were observed using photothermal Disperse Blue 14 dye.²⁷ Additionally, the temperature of AzoLCN films was monitored during the irradiation cycles (UV light: 2 minutes, light-off: 30 seconds). As shown in Fig. 4b, the temperature increase and decrease occur with a similar response time, approximately 6 seconds for a change in G' and < 5 seconds for a change in temperature. These results are all consistent with photothermal effects mainly driving the mechanical response observed. The versatility of the modulus

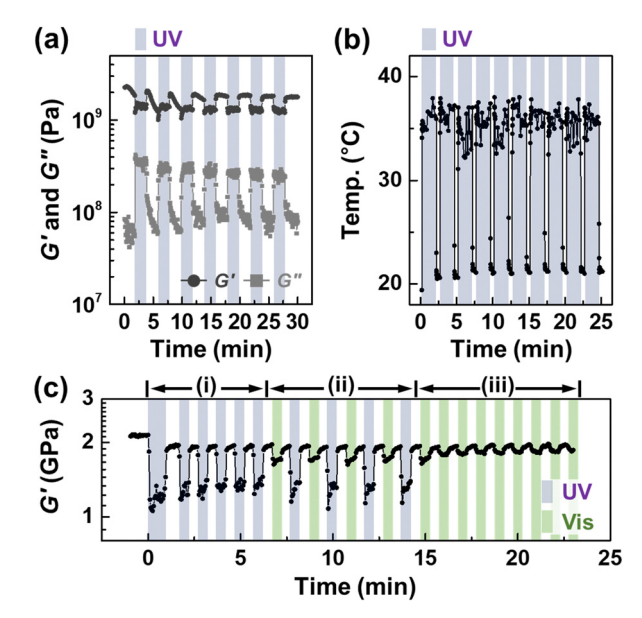


Fig. 4 (a) Storage and loss modulus and (b) temperature tracking of AzoLCN under alternative UV light irradiation on and off. (c) Storage modulus tracking of AzoLCN under a series of conditions (i: UV light on and off, ii: alternative UV and visible light on and off, iii: visible light on and off, at intervals of 30 s respectively).

change is demonstrated in Fig. 4c, where a series of reversible changes were achieved using both UV and visible light (Fig. S11, S12, ESI† and Fig. 4c). For these experiments, the DMA sample was illuminated with broadband visible light (380-700 nm) on one side and with UV light (365 nm) on the opposite side (Fig. S11, ESI†). For condition (i) (zero to 6.5 minutes), UV light was cycled between on and off state (30 second each). As seen by the DMA, quick and reversible oscillation in G' was observed, reaching a maximum value of ~1.25 GPa and a minimum value of ~ 1.1 GPa. The increase and decrease in storage modulus occurred within approximately 6 seconds (Fig. S12, ESI†). For condition (ii), an alternative irradiation cycle was conducted between UV and visible light with irradiation for 30 seconds, followed by 30 seconds interval without light. While there was a notable difference in the magnitude of changes between UV and visible light, both irradiation conditions resulted in a modulus decrease. For condition (iii), a modest change in G' was reversibly observed under repeated visible light irradiation (30 seconds each). While the response times are comparable to those in condition (i), the change in G'is less due to a reduced photothermal effect caused by visible light (Fig. S12, ESI†). Similar results were observed under constant irradiation with UV light and visible light pulses for 30 seconds or constant visible light irradiation and UV light pulses for 30 seconds (Fig. S13, ESI†). This reversibility of the mechanical property was affected by cross-linking density and oscillation speed (Fig. S14, ESI†). Additional explanation can be found in ESI.†

Fig. 5 summarizes the photothermal effect and changes in mechanical properties of the DA-based LCN. Initially, the Azocontaining LC network is in its thermodynamically most stable

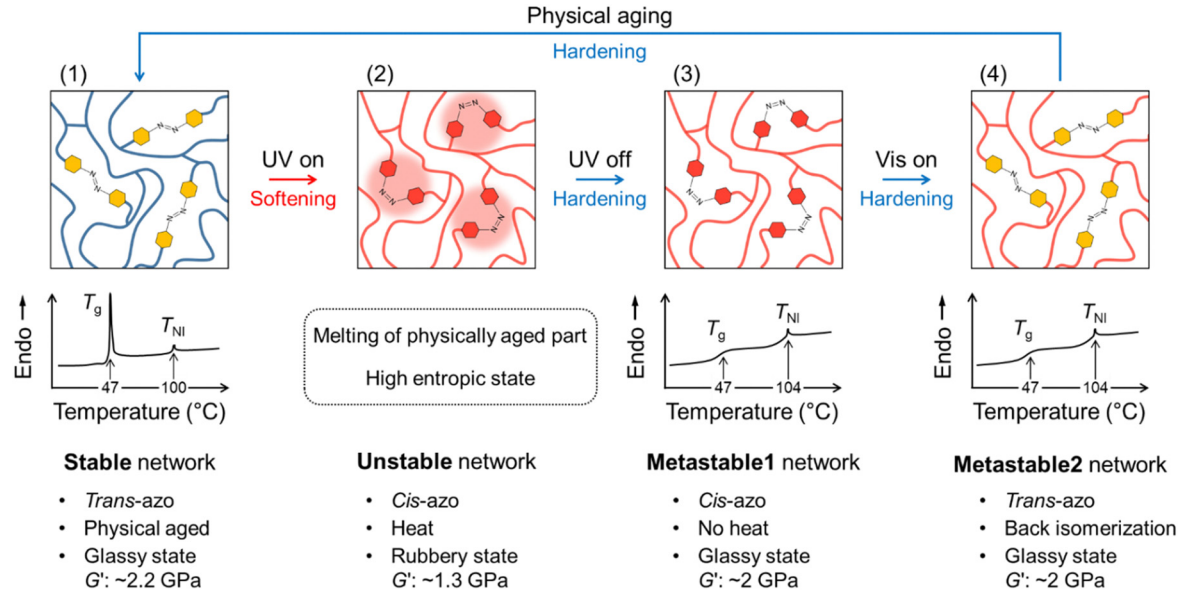


Fig. 5 Schematic illustration and summary of characteristic property changes of LC network on photothermal and photochemical effects.

state (1). This material is glassy and becomes physically aged over time, which is supported by the DSC data. In this state (1), the Azo isomer is the trans-isomer, densely packed, and exhibit the highest value in storage modulus (~ 2.2 GPa). Upon UV light irradiation, the temperature increases and photothermal softening occurs almost immediately, and the molecular azobenzene converts to the *cis*-isomer. This metastable state (2) exhibits a quasi-rubbery state, with a significant decrease in storage modulus (~1.3 GPa).²⁸ Under constant irradiation, a sustained rubber state is maintained. When the light is turned off, the material returns to the glassy state within seconds, and storage modulus is restored to ~ 2 GPa. From this state (3), conversion of the cis-isomer can occur thermally over a period of 5 hours or within seconds upon irradiation with visible light to afford state (4). Finally, state (1) can be recovered upon physical aging over an extended period of time (\sim 2 days).

Conclusions

In summary, we have developed a new photo-responsive liquid-crystal network by integrating readily available furan-functionalized azobenzene LC building block. Polydomain and monodomain AzoLCNs can be prepared under mild ambient conditions without the need for additives or UV light photocuring using a modular Diels-Alder cycloaddition methodology. The networks exhibit robust mechanical stiffness that can be reversibly modulated by 1 GPa by turning the UV light on and off. Through a comprehensive investigation of polydomain LCNs, it was found that photothermal softening predominantly governs the actuation performance of the LCNs. By adjusting the sequence of UV and Vis light irradiation, we achieved the ability to tune the modulus on demand. We believe this work will guide future developments of light-responsive LCNs.

Author contributions

CRediT: Minwook Park data curation (lead), formal analysis (lead), writing-original draft (lead); Jesus Guillen Campos methodology (equal), writing-review & editing (equal); Fredrick Stricker methodology (equal), writing-review & editing (equal); Javier Read de Alaniz formal analysis (equal), writing-review & editing (lead), supervision (lead).

Data availability

Data for this article entitled "Photo-responsive Diels-Alder Based Azobenzene-functionalized Main-chain Liquid Crystal Networks" are available at Dryad at DOI: https://doi.org/10.5061/dryad.jsxksn0jv. The temporary link can be shared during the peerreview process: Reviewer URL: https://datadryad.org/stash/share/AEfx_lwF6a_saOQGQEP-ahHf-7g1TpOKoT7BZwD8Mds.

Conflicts of interest

There are no conflicts to declare.

Acknowledgements

This work was primarily supported by the Office of Naval Research through a MURI on Photomechanical Material Systems (Grant No. ONR N00014-18-1-2624) with partial supported from the National Science Foundation (NSF) under Award No. EFMA-1935327.

Notes and references

D. C. Hoekstra, A. P. Schenning and M. G. Debije, *Soft Matter*, 2020, 16, 5106.

Paper

- 2 S. Pearson, J. Feng and A. del Campo, *Adv. Funct. Mater.*, 2021, **31**, 2105989.
- 3 J. Cui, D. M. Drotlef, I. Larraza, J. P. Fernández-Blázquez, L. F. Boesel, C. Ohm, M. Mezger, R. Zentel and A. del Campo, *Adv. Mater.*, 2012, 24, 4601–4604.
- 4 S. Dai, P. Ravi and K. C. Tam, Soft Matter, 2008, 4, 435-449.
- 5 E. Smela, O. Inganäs and I. Lundström, *Science*, 1995, 268, 1735–1738.
- 6 Y. Li, O. Rios, J. K. Keum, J. Chen and M. R. Kessler, ACS Appl. Mater. Interfaces, 2016, 8, 15750-15757.
- 7 K. M. Herbert, H. E. Fowler, J. M. McCracken, K. R. Schlafmann, J. A. Koch and T. J. White, *Nat. Rev. Mater.*, 2022, 7, 23–38.
- 8 J. Gao, M. Tian, Y. He, H. Yi and J. Guo, *Adv. Funct. Mater.*, 2022, **32**, 2107145.
- T. S. Hebner, M. Podgórski, S. Mavila, T. J. White and C. N. Bowman, *Angew. Chem., Int. Ed.*, 2022, 61, 202116522.
- 10 J. Guillen Campos, F. Stricker, K. D. Clark, M. Park, S. J. Bailey, A. J. Kuenstler, R. C. Hayward and J. Read de Alaniz, Angew. Chem., Int. Ed., 2023, 62, 202214339.
- 11 A. Ryabchun, Q. Li, F. Lancia, I. Aprahamian and N. Katsonis, J. Am. Chem. Soc., 2019, 141, 1196–1200.
- 12 H. K. Bisoyi, A. M. Urbas and Q. Li, Adv. Opt. Mater., 2018, 6, 1800458.
- 13 X. Lu, S. Guo, X. Tong, H. Xia and Y. Zhao, *Adv. Mater.*, 2017, **29**, 1606467.
- 14 M. Park, F. Stricker, J. Guillen Campos, K. D. Clark, J. Lee, Y. Kwon, M. T. Valentine and J. Read de Alaniz, ACS Macro Lett., 2022, 12, 33–39.

- 15 M. Del Pozo, J. A. Sol, A. P. Schenning and M. G. Debije, *Adv. Mater.*, 2022, **34**, 2104390.
- 16 H. Shahsavan, L. Yu, A. Jákli and B. Zhao, Soft Matter, 2017, 13, 8006–8022.
- 17 T. Ohzono, H. Minamikawa, E. Koyama and Y. Norikane, *Adv. Mater. Interfaces*, 2021, **8**, 2100672.
- 18 T. Takeshima, W. Y. Liao, Y. Nagashima, K. Beppu, M. Hara, S. Nagano and T. Seki, *Macromolecules*, 2015, 48, 6378–6384.
- 19 M. Park, D. G. Kang, W. J. Yoon, Y. J. Choi, J. Koo, S. I. Lim, S. K. Ahn and K. U. Jeong, *Chem. Mater.*, 2019, 32, 166–172.
- D. J. Mulder, T. Liang, Y. Xu, J. ter Schiphorst, L. M. Scheres,
 B. M. Oosterlaken, Z. Borneman, K. Nijmeijer and
 A. P. Schenning, J. Mater. Chem. C, 2018, 6, 5018–5024.
- 21 T. Ikeda, M. Nakano, Y. Yu, O. Tsutsumi and A. Kanazawa, *Adv. Mater.*, 2003, **15**, 201–205.
- 22 B. R. Donovan, H. E. Fowler, V. M. Matavulj and T. J. White, Angew. Chem., Int. Ed., 2019, 58, 13744–13748.
- 23 M. Kondo, Y. Yu and T. Ikeda, Angew. Chem., Int. Ed., 2006, 45, 1378–1382.
- 24 J. Vapaavuori, A. Laventure, C. G. Bazuin, O. Lebel and C. Pellerin, J. Am. Chem. Soc., 2015, 137, 13510–13517.
- 25 K. M. Lee, H. Koerner, D. H. Wang, L. S. Tan and T. J. White, *Macromolecules*, 2012, 45, 7527–7534.
- 26 Z. C. Jiang, Y. Y. Xiao, L. Yin, L. Han and Y. Zhao, Angew. Chem., 2020, 132, 4955–4961.
- 27 J. E. Marshall and E. M. Terentjev, Soft Matter, 2013, 9, 8547–8551.
- 28 X. Huang, L. Qin, J. Wang, X. Zhang, B. Peng and Y. Yu, *Adv. Funct. Mater.*, 2022, 32, 2208312.